

By acceptance of this article, the publisher or recipient acknowledges the U.S. Government's right to retain a nonexclusive, royalty-free license in and to any copyright covering the article.

STATISTICAL TECHNIQUES FOR AUTOMATING THE DETECTION OF ANOMALOUS PERFORMANCE IN ROTATING MACHINERY*

K. R. Piety, T. E. Magette**

Oak Ridge National Laboratory
Oak Ridge, Tennessee 37830

*Research sponsored by the Division of Reactor Research and Technology, U.S. Department of Energy, under contract W-7405-eng-26 with the Union Carbide Corporation.

**Nuclear Engineering Department, University of Tennessee, Knoxville 37919.

MASTER

OAK RIDGE NATIONAL LABORATORY
Oak Ridge, Tennessee 37830
Operated by
UNION CARBIDE CORPORATION
for the
U.S. DEPARTMENT OF ENERGY

NOTICE
This report was prepared as an account of work sponsored by the United States Government. Neither the United States nor the United States Department of Energy, nor any of their employees, nor any of their contractors, subcontractors, or their employees, makes any warranty, express or implied, or assumes any legal liability or responsibility for the accuracy, completeness or usefulness of any information, apparatus, product or process disclosed, or represents that its use would not infringe privately owned rights.

STATISTICAL TECHNIQUES FOR AUTOMATING THE DETECTION OF
ANOMALOUS PERFORMANCE IN ROTATING MACHINERY*

K. R. Piety
Oak Ridge National Laboratory
Oak Ridge, Tennessee 37830

T. E. Magette
Nuclear Engineering Department
University of Tennessee, Knoxville 37919

Kenneth R. Piety has recently joined the technical staff at Technology for Energy Corporation where his principal activities include the design of automated measurement and control systems and field measurement services. Previously, he was employed at the Oak Ridge National Laboratory where he developed automated surveillance systems for nuclear reactors and rotating equipment. He is a graduate of the University

of Tennessee and holds a Ph.D. in nuclear engineering.

ABSTRACT

We have assessed the level of technology utilized in automated systems that monitor industrial rotating equipment and the potential of alternative surveillance methods. We conclude that changes in surveillance methodology would upgrade ongoing programs and yet still be practical for implementation. We formulated an improved anomaly recognition methodology and implemented these methods on a minicomputer system. The effectiveness of our monitoring system was evaluated in laboratory tests on a small rotor assembly, using vibrational signals from both displacement probes and accelerometers. Time and frequency domain descriptors are selected to compose an overall signature that characterizes the monitored equipment. Limits for normal operation of the rotor assembly are established automatically during an initial learning period. Thereafter, anomaly detection is accomplished by applying an approximate statistical test to each signature descriptor. As demonstrated over months of testing, this monitoring system is capable of detecting anomalous conditions while exhibiting a false alarm rate below 0.5%.

INTRODUCTION

Scope of the work: The purpose of this work is the demonstration of surveillance techniques that can extend the performance capabilities of automated systems for monitoring industrial rotating equipment. In preparation for this work we

*Research sponsored by the Division of Reactor Research and Technology, U.S. Department of Energy, under contract W-7405-eng-26 with the Union Carbide Corporation.

have assessed the effectiveness of ongoing monitoring programs and the potential improvements offered by alternative programs. Based on our evaluation of the merits and deficiencies in existing and proposed surveillance systems, we formulated an improved anomaly recognition methodology. The monitoring system implemented and tested at ORNL offers improved monitoring performance, utilizing methods that are practical for even large industrial applications.

Background: The practice of monitoring gross vibrational levels as an indication of machinery health began more than 150 years ago. However, it was not until 1939 that vibration sensors and rudimentary signal analysis techniques enabled the compilation of empirical vibrational severity criteria (1-3). Only in the past 25 years have advancements in data processing techniques and computer hardware allowed machinery health to be evaluated using signatures derived from the detailed structure of vibrational signals (4,5).

Although the advantages of signature analysis techniques are widely acknowledged, the demands such analytical methods place on plant personnel limit the use of such techniques for general surveillance tasks (5,6). Computer automation of these monitoring requirements alleviates this drawback and allows maintenance personnel to direct their efforts towards equipment most in need of attention. Additionally, a computerized surveillance system should provide sufficient sensitivity to give early warning of incipient failures, thus enhancing diagnostic capabilities and allowing better scheduling of maintenance. However, while monitoring of machinery to detect excessive vibration is a well-established practice, a best approach for automating such monitoring activities has not gained general acceptance.

Limitations of monitoring systems: There are certain drawbacks associated with all systems presently used for on-line surveillance of rotating equipment. The most basic of such systems are those which derive a set of parameters characterizing the vibration signal (such as its peak-to-peak amplitude, RMS power, or power at the rotational frequency) for comparison with absolute limits (7-9). To set such limits one must resort to a vibration severity chart, perform analytical calculations for the equipment to be monitored, or accumulate the necessary information from testing. Since fixed limits must encompass the "worst-case" conditions over the entire range of normal operations, sensitivity to anomalous performance at any given operational state is reduced (9,10). Another disadvantage frequently associated with this approach is a lack of information on which to base diagnostic decisions (9,11) once an anomaly has been detected.

To compensate for this deficiency some monitoring systems add trending capabilities or utilize the detail available with complete spectral analysis (12-16). Unfortunately, due to the storage limitations which exist in systems monitoring several hundred data channels, trending the entire power spectrum is typically not practical. The storage problems associated with maintaining full spectral detail are further compounded if baseline signatures and limiting criteria are to be saved as a function of operational conditions. A common compromise is to trend only gross vibrational levels and to alarm if these parameters exceed acceptable limits. The complete power spectra of the vibrational signals are saved only at baseline conditions at the outset of monitoring, with further spectral analysis performed only upon operator request, at widely spaced intervals, or under alarm conditions. A decision to monitor only gross vibrational level sacrifices sensitivity (6,11,17). However, the decision to monitor a larger set of detailed descriptors makes it difficult to establish meaningful detection criteria (particularly as a function of operational conditions) and has, in some cases, exhausted the patience of operations personnel (7).

Another approach taken by some researchers is the implementation of statistical algorithms as a basis for anomaly detection (17-19). Both the experience and success in applying these techniques have been limited. Our own previous efforts with a strictly statistical approach revealed that the rotating equipment being monitored was nonstationary. Even at fixed conditions, the equipment would operate for indefinite periods described by one set of statistical parameters and then would randomly change to other equally normal conditions with different statistics. Data taken under such conditions results in biased samples of the statistical populations, thereby destroying the rigor of statistical tests (19). Statistical techniques can also be data intensive and thus become unmanageable with the added complication of varying operational conditions.

The most mathematically complex techniques envisioned for automated surveillance systems may be generally referred to as pattern recognition methods (17, 20-22). Implementation of these methods typically requires accumulation of signatures for abnormal conditions in addition to those for normal conditions. Such comprehensive data requirements cannot normally be satisfied, particularly at the onset of surveillance activities. In addition, since pattern recognition methods have characteristically been developed for other applications, they rarely incorporate — and then only indirectly — engineering knowledge pertinent to specific surveillance tasks. Nonetheless, it would appear that some of these methods do show promise as diagnostic algorithms once the required data is obtained.

THE ORNL SURVEILLANCE SYSTEM

Overview: This monitoring system is the result of applying engineering judgment to the specific task of automating machinery surveillance.

To maintain high sensitivity to anomalies, vibrational signatures are catalogued as a function of operational conditions, and detection decisions are based on simple statistical tests. The determination of alarm criteria is accomplished automatically, based upon normal data obtained during a learning period. Judicious feature selection is incorporated to reduce storage requirements; however, data logging adequate for diagnostic investigations is provided. False alarms are reduced by implementing processing logic that compensates for normal data variations.

Feature selection: A vibration signature is obtained by selecting only a subset of the various signal descriptors that might be derived from the measured data. This selection process introduces available engineering knowledge related to individual equipment, critical fault events, or the signal character into the monitoring system. For example, the power in the fifth order (five times the rotational speed) would logically be included as a feature describing a fan with five blades. Obviously, the specific set of parameters comprising a signature will vary for dissimilar applications. Discarding or combining redundant descriptors should result in a reduced set of descriptors which enhance the information content of the measured data. For our test purposes we chose 48 parameters per signal which define the phase, size, and shape of the time-averaged waveform, the total power of the signal, the harmonic and nonharmonic power, the power and phase of the first three orders of rotation, the spectrum-weighted order, and the average harmonic and nonharmonic order. A detailed explanation of these descriptors is given in the appendix. Although these features are not proposed as an optimum set for other monitoring applications, many descriptors in widespread use are included, and the ability to compare the performance of descriptors with different levels of detail is provided.

Reference catalogue of baseline data: Baseline signatures are catalogued as a function of operational conditions. This procedure necessitates access to variables that define the operational state, for example, speed, load, or flow. Discrete intervals are chosen to span the full range available to controlling variables; once specified, the interval structure determines the maximum number of entries required in the reference catalogue. Since it has been demonstrated that variations in speed and load can introduce changes in vibration exceeding those associated with anomalies (10), compensation for such changes stimulated by control variables is necessary for maintaining sensitivity for anomaly detection and for reducing false alarms. Although most investigations support this conclusion (7-10), few monitoring systems implement capabilities for handling this complication. We chose the direct cataloguing approach after reviewing various mathematical alternatives and experimenting with techniques based on principal components analysis and regression analysis.

Establishing limiting criteria: Baseline signatures and their normal interval of variation

are established automatically by observing equipment operation during an initial learning period. During this period, the equipment must be operated at or near all conditions for which monitoring capability will be needed. The learning period should be of sufficient duration to include a representative sample of normal variations. This period was 2-4 days in our investigations. The adequacy of learning appears to be more closely related to elapsed clock time than to the number of signatures measured, because of the biased sampling previously cited (19). Several checks are available to ascertain if the learning period has been adequate. These include counters which conservatively estimate the proportion of the learning signatures considered normal and the number of learning signatures since the last abnormal classification, as well as the ability to switch to the monitoring mode for a defined period during which a detailed monitoring summary is automatically obtained. If necessary, additional learning can be initiated at any time. Since the system detects deviations from whatever baselines are established, sensitivity to further degradation is maintained whether or not equipment was operating normally during the learning period.

Detection logic: During monitoring, each vibration signature is measured under steady operating conditions and tested to determine if its deviations from the baseline signatures are statistically significant. While the application of classical statistics is invalidated by biased sampling and by lumping differing operations into coarse intervals, the deviations calculated in approximate standard deviation units do provide a quantitative measure of problem severity. Approximate methods of calculating signature deviations, although lacking in mathematical elegance, are incorporated because they have proven to reduce the incidence of false alarms.

During learning, the maximum and minimum values encountered for every feature are stored for each operational interval. When a signature at a given operational state is tested, the extreme values normal to that operational interval and those values from its nearest neighbors are combined to obtain a smeared interval that encloses all extremes. From this interval, a pseudo mean, m , and a pseudo standard deviation, σ , are calculated as follows:

$$m = \frac{\text{Max} + \text{Min}}{2}$$

$$\sigma = \frac{\text{Max} - \text{Min}}{6}$$

The absolute deviations calculated using these quantities are compared against a confidence limit which decreases from $C + 3$ to C (an input parameter) as the number of measurements, M , upon which m and σ are based, increases from 0 to 500:

$$\left| \frac{x - m}{\sigma} \right| < C + 3 \left(\frac{500 - M}{500} \right)$$

Statistical intuition and experience indicate that a value of $C \approx 7$ is most appropriate. For industrial surveillance applications, testing the gross

vibration levels against established severity criteria (1-4) is also recommended. This additional detection capability would provide limited protection during learning when no other performance monitoring is in force and would inherently set an upper limit on the statistically derived criteria.

Comprehensive data logging for diagnosis: No automatic diagnostic logic is implemented in this system. However, the detection of anomalous events does automatically initiate procedures that log data to assist in diagnosis. If a signature is encountered that exceeds normal bounds, an anomaly signature catalogue is begun for all signals from the suspect machine. The anomaly catalogue allows detailed comparisons between data accumulated following the suspect event with that in the baseline reference catalogue obtained during learning. Additionally, a detection summary which tallies suspect events for each signature component and computes the average deviation is collected and available on request. Also upon demand, a variety of visual displays from standard signal processing algorithms (orbits and detailed power spectra) can be obtained, although data from these analysis capabilities are not automatically retained. It is expected that the data collected for diagnostic purposes will allow the development of algorithms to diagnose the most probable faults.

RESULTS

Software implementation: The surveillance software has been implemented on a Digital Equipment Corp., PDP 11/34 minicomputer with 28K words of memory. Mass storage capability is provided by two disks, each with a 1.2M word capacity. All programs are written in FORTRAN except for the peripheral handler routines that require assembly language.

A small portion of the disk storage is required for the software system; the remaining portion, ~2M words, is available for data storage. The burden of the data storage is associated with cataloguing baseline data. The total storage requirement, R , for this reference catalogue is given by

$$R = 4 \sum_{i=1}^M O_i \sum_{j=1}^{S_i} D_{ij}$$

where M is the number of machines to be monitored; O_i , the number of lumped operational states allowed for the i th machine; S_i , the number of sensors on the i th machine; and D_{ij} , the number of descriptors used to describe the information from the j th sensor on the i th machine.

The mass storage requirements for the monitoring system are within reason for even large-scale industrial applications. Assume, for example, that one desired to monitor 100 machines, each equipped with eight sensors. An analysis that assigns 20 lumped operational states to each machine and characterizes each signal with 25 descriptors would require 1.6M words of storage. This allows one to

describe each piece of equipment with 200 descriptors and still reserve some storage area for logging diagnostic data.

Evaluation of monitoring system: A laboratory evaluation of the monitoring software has been accomplished using a small rotor assembly driven by a fractional horsepower motor.* Three displacement probes and two accelerometers are installed on the rotor as shown in Fig. 1. One probe ("keyphasor") provides a tach signal and, through supplementary electronics, generates a rotationally synchronized sampling pulse to trigger the analog-to-digital converter. Two other probes, placed at 90° to each other, measure the radial vibration of the shaft. In addition, two accelerometers are installed on the inboard bearing housing to measure the orthogonal components of radial vibration. In our tests, two signatures describing rotor operation are actually calculated, one for the displacement probes and the other for the accelerometers. Each signature is composed from descriptors for both the horizontal and vertical directions.

The rotor can attain speeds from 0 to 200 revolutions per second (rps); this was the only control variable altered during our tests. Lumped operational states were defined in 1-rps intervals. This speed resolution was a convenient choice which offered reasonable detail.

In our previous work (19), the monitoring system was unable to maintain a low false alarm rate over extended periods of testing using the limiting criteria which were automatically established. This difficulty was overcome by modifying the detection logic and by extending the learning period. We have, in fact, demonstrated that a learning file composed in a few days can be used to monitor normal operation for periods of several months without false alarms becoming a difficulty.

The detection capability of the monitoring system was investigated by purposely introducing fault conditions into the test setup. The four fault types chosen were shaft rub, imbalance, mechanical looseness, and misalignments. Each anomaly type could be introduced in varying degrees of severity. Some faults introduced no discernible perturbation to the vibration signals; however, detection was always possible as the severity level was increased. After the anomalous conditions associated with fault testing were removed, the return to normal operation was verified by the monitoring system. Examples of the type of diagnostic data available from the system are presented as the individual tests are described.

Imbalance test: The balance of the rotor was altered by the addition of a 1.52-g mass 3.32 cm from the shaft centerline (translating to an imbalance force of 0.238 Nt m at 60 rps). The change in the vibration was readily detected by both horizontal and vertical displacement probes, as illustrated by the detection summary shown in Table 1. Any signature for which some descriptor was out of

normal bounds is considered suspect. This was the case for all 1000 comparison signatures of each type comprising this summary. An interesting detail in this test is that the weight added actually improved the balance of the rotor. This can be seen in both Fig. 2, which shows the time-averaged orbit for both baseline and imbalance conditions, and in the detection summary, which shows a reduction (negative deviation) in the signal descriptors associated with the amplitude of the vibration. A change in vibrational amplitude at the first order is well established as the primary indication of changes in balance. However, as noted in Table 1, this descriptor was affected less dramatically than others. This results from the asymmetric domain (always positive) of power descriptors which reduces their statistical sensitivity to reductions in their magnitude. This can be corrected by using the log of their magnitudes. The phase of the first order does show significant variations throughout the entire speed range, as demonstrated in Fig. 3. The peak displacement was also significantly altered by the imbalance; Fig. 4 contrasts normal and anomalous variations for the peak displacement descriptor as a function of speed.

Misalignment test: The alignment of the rotor can be altered by placing shims under the bearing pedestals. The data shown resulted from raising one side of the inboard bearing pedestal by 1.32 mm, thus offsetting the centerlines of the motor and rotor shafts. This misalignment was readily detected, as indicated by most of the descriptors shown in Table 2. Unexpectedly, all descriptors except nonharmonic power showed a decrease in their magnitudes. Figure 5 shows this effect in detail for the power at the second order and is in contrast to Fig. 6 which shows the increase in the nonharmonic power.

The decrease in overall and harmonic vibration levels was not, however, an indication that the damage potential had been reduced, since the coupling to the motor destructively failed within 12 hours. The prominent peak in the plot of nonharmonic power, Fig. 6, resulted from data taken just prior to the destruction of the coupling. A reduction in vibration levels was not common to all misalignment tests; nonetheless, this case should serve to caution system designers that would ignore the importance of such effects.

Mechanical looseness test: This test was accomplished by loosening the screws that fasten the inboard bearing pedestal to the base plate. In this case, the accelerometers had a greater sensitivity to the abnormality than did the proximity probes. The rather pronounced effect on the accelerometer signatures, tabulated in the detection summary given in Table 3, most likely resulted from altering the mechanical impedance at the bearing pedestal (23). All descriptors influenced by the harmonic content of the signal were strongly affected. A plot of the extreme values experienced under both normal and loose conditions for the power at the second order as a function of speed is shown in Fig. 7.

*Bently Nevada Corp., Minden, Nevada, Model RK-3.

Partial shaft rub test: In our tests, the presence of shaft rubs was indicated most strongly by the accelerometer signals. The data shown in Table 4 are from a partial shaft rub, where the rub screw (see Fig. 1) was allowed to lightly bounce against the shaft. This anomaly emphasizes again the importance of choosing descriptors which measure nonharmonic signal power (11). As seen from the detection summary (Table 4), the nonharmonic power is the only parameter which dependably indicates the presence of the rub. Detailed power spectra for the accelerometer under normal and rub conditions are shown in Figs. 8 and 9, respectively. The noise floor of the rub spectrum is raised over a rather broad order interval; this trait has been characteristic of rub anomalies we tested.

SUMMARY AND RECOMMENDATIONS

The monitoring system automatically established limiting criteria during an initial learning period of a few days; subsequently, while monitoring the test rotor during several months of normal operation, the system experienced a false alarm

rate of ~0.5%. At the same time, the monitoring system successfully detected all fault types introduced into the test setup. Tests on "real-world" equipment are needed to provide final verification of the monitoring techniques. The incremental expense required to implement hardware for this purpose would be small in an industrial plant where sensors, electronics, and cabling already exist for vibration monitoring. Furthermore, the data required to make this monitoring approach effective would not hinder normal industrial operations.

There are areas that could benefit from additional investigation in the laboratory environment. A comparison of the relative values of alternative descriptors under given fault conditions would be worthwhile. This should be pursued in conjunction with extending the set of fault types available, e.g., bearing problems. Other tests should examine the effects of using fewer (more coarse) intervals to define the lumped operational states. Finally, techniques to diagnose the most probable fault should be developed by drawing upon the extensive data automatically logged by the monitoring system.

Table 1. Detection summary (1000 signatures tested) for imbalance test over the speed range of 60 to 85 rps.

Signature Descriptor	Displacement Signature		Acceleration Signature	
	X Sensor No. Out (Dev. ^a)	Y Sensor No. Out (Dev. ^a)	X Sensor No. Out (Dev. ^a)	Y Sensor No. Out (Dev. ^a)
Lag values	997	802	994	0
Shape factor	0	8	0	0
Size factor	416 (-12.2)	1 (-18.9)	0 (0.0)	0 (0.0)
Peak values	416 (-10.4)	1 (-26.3)	0 (0.0)	0 (0.0)
Total power	81 (-10.6)	1 (-18.6)	0 (0.0)	0 (0.0)
Harmonic power	81 (-10.6)	1 (-18.6)	0 (0.0)	0 (0.0)
Nonharmonic power	0 (0.0)	0 (0.0)	0 (0.0)	0 (0.0)
Average order	350 (8.7)	18 (12.5)	95 (8.0)	0 (0.0)
Average harmonic order	38 (8.9)	12 (11.8)	1 (7.5)	0 (0.0)
Average nonharmonic order	0 (0.0)	0 (0.0)	0 (0.0)	0 (0.0)
PSD order 1	71 (-10.9)	1 (-18.6)	0 (0.0)	0 (0.0)
PSD order 2	0 (0.0)	1 (-8.5)	0 (0.0)	0 (0.0)
PSD order 3	0 (0.0)	0 (0.0)	0 (0.0)	0 (0.0)
Phase order 1	1000	416	1000	0
Phase order 2	726	914	445	0
Phase order 3	11	10	409	0
	No. of suspect signatures = 1000		No. of suspect signatures = 1000	

^a Deviations from baseline data in approximate standard deviation units.

Table 2. Detection summary (500 signatures tested) for misalignment test over the speed range of 55 to 100 rps.

Signature Descriptor	Displacement Signature		Acceleration Signature	
	X Sensor No. Out (Dev. ^a)	Y Sensor No. Out (Dev. ^a)	X Sensor No. Out (Dev. ^a)	Y Sensor No. Out (Dev. ^a)
Lag values	426	336	487	0
Shape factor	0	13	0	0
Size factor	463 (-18.1)	51 (-18.4)	2 (-8.8)	0 (0.0)
Peak values	310 (-13.7)	47 (-11.0)	0 (0.0)	0 (0.0)
Total power	313 (-13.1)	47 (-16.4)	0 (0.0)	0 (0.0)
Harmonic power	315 (-13.7)	47 (-18.7)	0 (0.0)	0 (0.0)
Nonharmonic power	459 (333.9)	461 (514.3)	38 (10.0)	0 (0.0)
Average order	23 (3.5)	6 (-10.7)	179 (10.4)	0 (0.0)
Average harmonic order	11 (9.6)	7 (18.7)	101 (14.4)	0 (0.0)
Average nonharmonic order	0 (0.0)	0 (0.0)	408 (-14.2)	14 (-8.3)
PSD order 1	315 (-13.7)	47 (-18.7)	5 (20.5)	0 (0.0)
PSD order 2	101 (-9.1)	47 (-8.3)	0 (0.0)	0 (0.0)
PSD order 3	10 (27.0)	11 (18.0)	14 (35.0)	0 (0.0)
Phase order 1	493	327	496	3
Phase order 2	1	189	22	0
Phase order 3	28	305	336	1
No. of suspect signatures = 500		No. of suspect signatures = 500		

^aDeviations from baseline data in approximate standard deviation units.

Table 3. Detection summary (1000 signatures tested) for mechanical looseness test over the speed range of 75 to 95 rps.

Signature Descriptor	Displacement Signature		Acceleration Signature	
	X Sensor No. Out (Dev. ^a)	Y Sensor No. Out (Dev. ^a)	X Sensor No. Out (Dev. ^a)	Y Sensor No. Out (Dev. ^a)
Lag values	0	5	194	0
Shape factor	0	0	0	0
Size factor	7 (-8.6)	0 (0.0)	0 (0.0)	26 (9.9)
Peak values	8 (-9.0)	0 (0.0)	151 (9.8)	309 (17.1)
Total power	7 (-8.4)	0 (0.0)	137 (9.7)	210 (17.3)
Harmonic power	7 (-8.5)	0 (0.0)	114 (10.1)	313 (17.0)
Nonharmonic power	47 (24.9)	6 (9.9)	121 (15.8)	96 (16.1)
Average order	0 (0.0)	0 (0.0)	13 (9.1)	0 (0.0)
Average harmonic order	0 (0.0)	0 (0.0)	7 (9.1)	0 (0.0)
Average nonharmonic order	0 (0.0)	0 (0.0)	341 (-11.3)	15 (7.9)
PSD order 1	7 (-8.5)	0 (0.0)	0 (0.0)	112 (13.2)
PSD order 2	0 (0.0)	0 (0.0)	957 (154.0)	216 (21.5)
PSD order 3	0 (0.0)	3 (0.0)	901 (126.8)	131 (16.3)
Phase order 1	0	29	353	0
Phase order 2	0	32	419	0
Phase order 3	0	0	266	0
No. of suspect signatures = 87		No. of suspect signatures = 1000		

^aDeviations from baseline data in approximate standard deviation units.

Table 4. Detection summary (20 signatures tested) for partial shaft rub test over the speed range of 60 to 65 rps.

Signature Descriptor	Displacement Signature		Acceleration Signature	
	X Sensor No. Out (Dev. ^a)	Y Sensor No. Out (Dev. ^a)	X Sensor No. Out (Dev. ^a)	Y Sensor No. Out (Dev. ^a)
Lag values	0	0	0	0
Shape factor	0	0	0	0
Size factor	0 (0.0)	0 (0.0)	0 (0.0)	0 (0.0)
Peak values	0 (0.0)	0 (0.0)	0 (0.0)	20 (27.1)
Total power	0 (0.0)	0 (0.0)	0 (0.0)	15 (17.9)
Harmonic power	0 (0.0)	0 (0.0)	0 (0.0)	0 (0.0)
Nonharmonic power	4 (26.4)	17 (85.7)	19 (19.4)	20 (30.8)
Average order	0 (0.0)	0 (0.0)	0 (0.0)	0 (0.0)
Average harmonic order	0 (0.0)	0 (0.0)	0 (0.0)	0 (0.0)
Average nonharmonic order	0 (0.0)	0 (0.0)	0 (0.0)	0 (0.0)
PSD order 1	0 (0.0)	0 (0.0)	0 (0.0)	0 (0.0)
PSD order 2	0 (0.0)	0 (0.0)	0 (0.0)	0 (0.0)
PSD order 3	0 (0.0)	0 (0.0)	0 (0.0)	0 (0.0)
Phase order 1	0	0	0	0
Phase order 2	0	0	0	0
Phase order 3	0	1	0	0
No. of suspect signatures = 17		No. of suspect signatures = 20		

^aDeviations from baseline data in approximate standard deviation units.

Fig. 1. The rotor assembly used in testing the monitoring system.

Fig. 2. The time-averaged orbits for normal and imbalance conditions.

Fig. 3. The range of phase values (displacement probe) at the first order for normal and imbalance conditions vs speed.

Fig. 4. The range of peak displacements for normal and imbalance conditions vs speed.

Fig. 5. The range of power estimates (displacement probe) at the second order for normal and misaligned conditions vs speed.

Fig. 6. The range of nonharmonic power estimates (displacement probe) for normal and misaligned conditions vs speed.

Fig. 7. The range of power estimates (accelerometer) at the second order for normal and mechanically loose conditions vs speed.

Fig. 8. Power spectrum of horizontal accelerometer during normal rotor operation at 59 rps.

Fig. 9. Power spectrum of horizontal accelerometer during partial shaft rub test at 59 rps.

ORNL DWG 78-17963

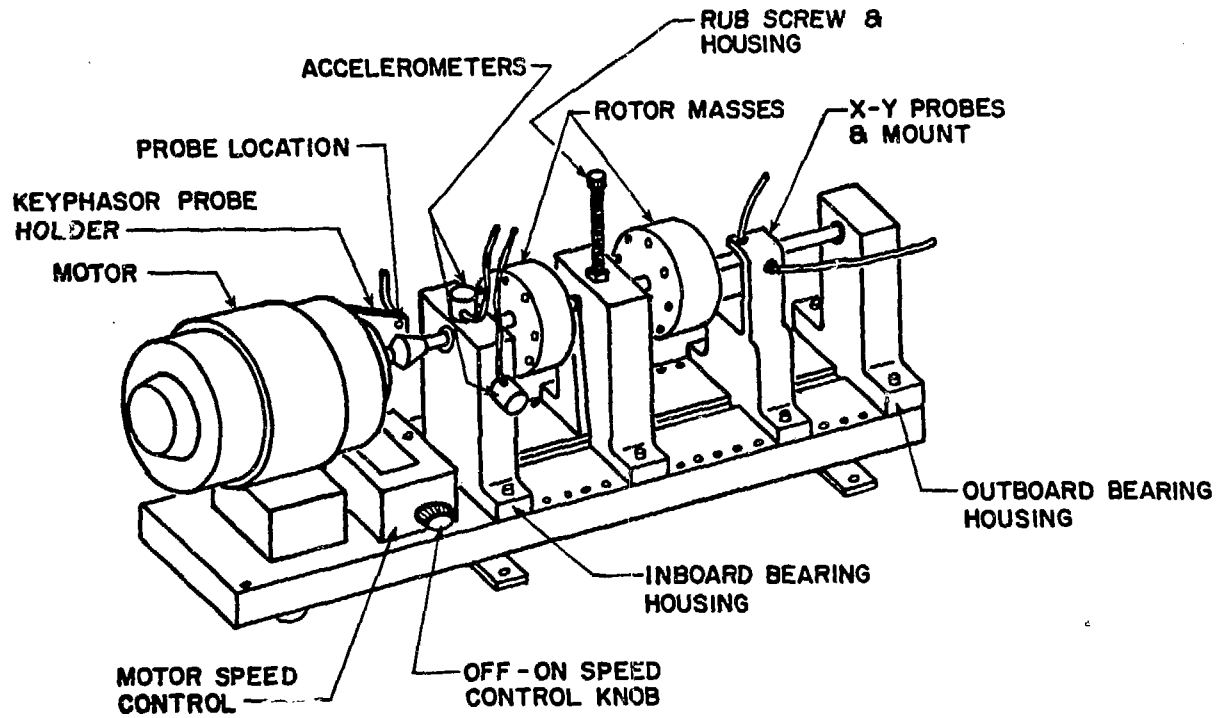
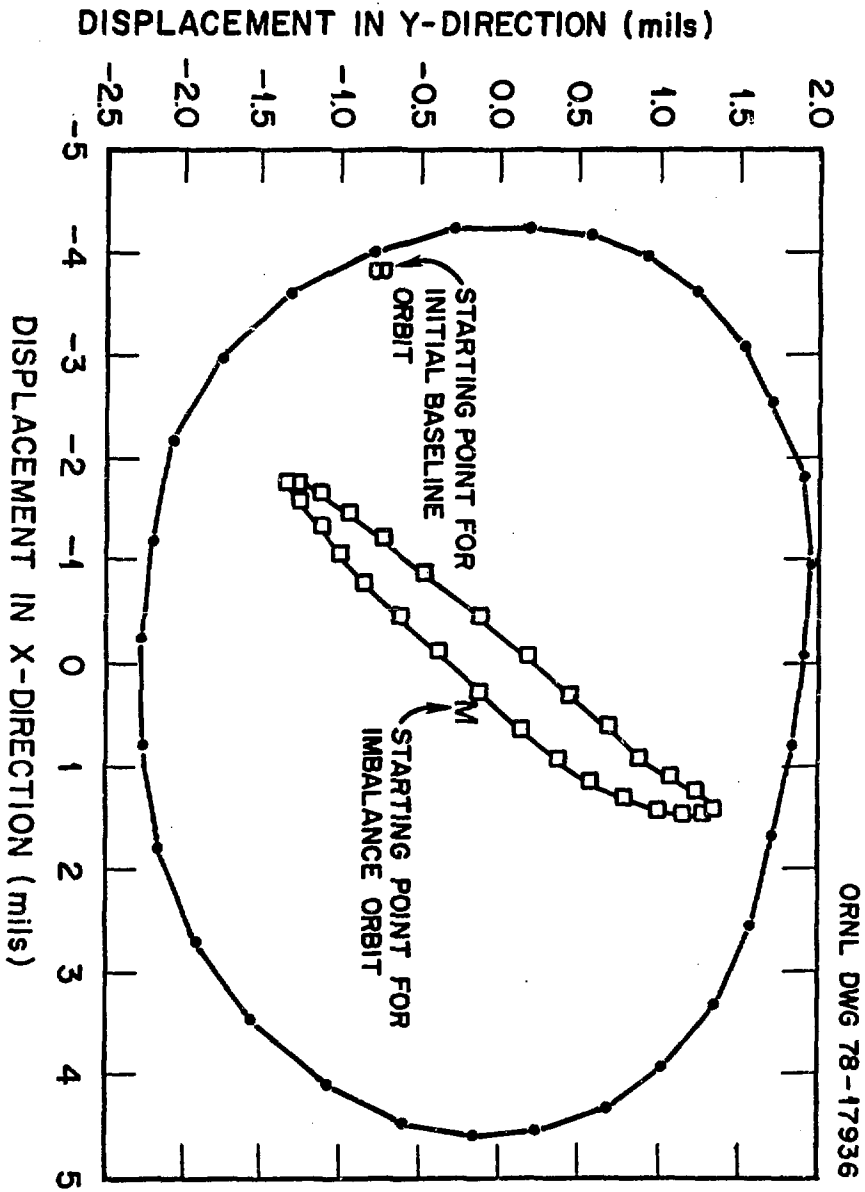
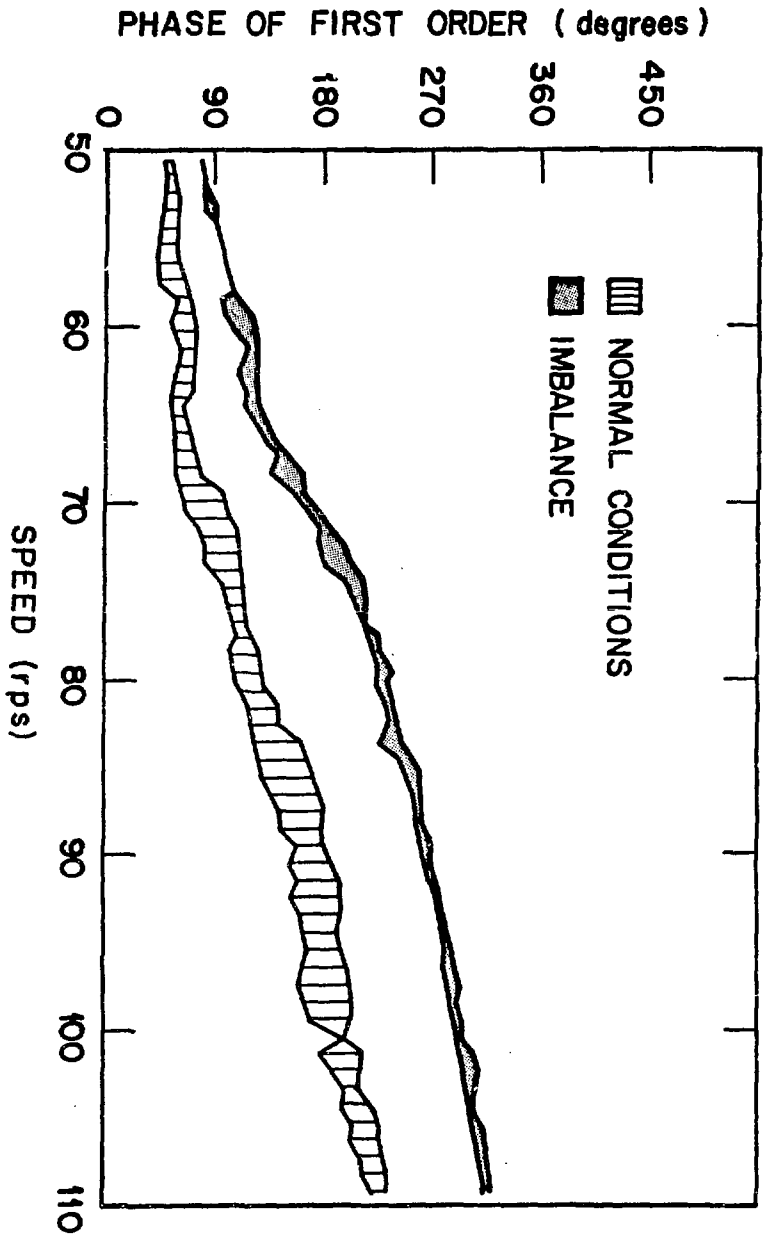


Fig. 1. The rotor assembly used in testing the monitoring system.



ORNL DWG 78-17936

Fig. 2. The time-averaged orbits for normal and imbalance conditions.



ORNL DWG 78-17943

Fig. 3. The range of phase values (displacement probe) at the first order for normal and imbalance conditions vs speed.

ORNL DWG 78-17942

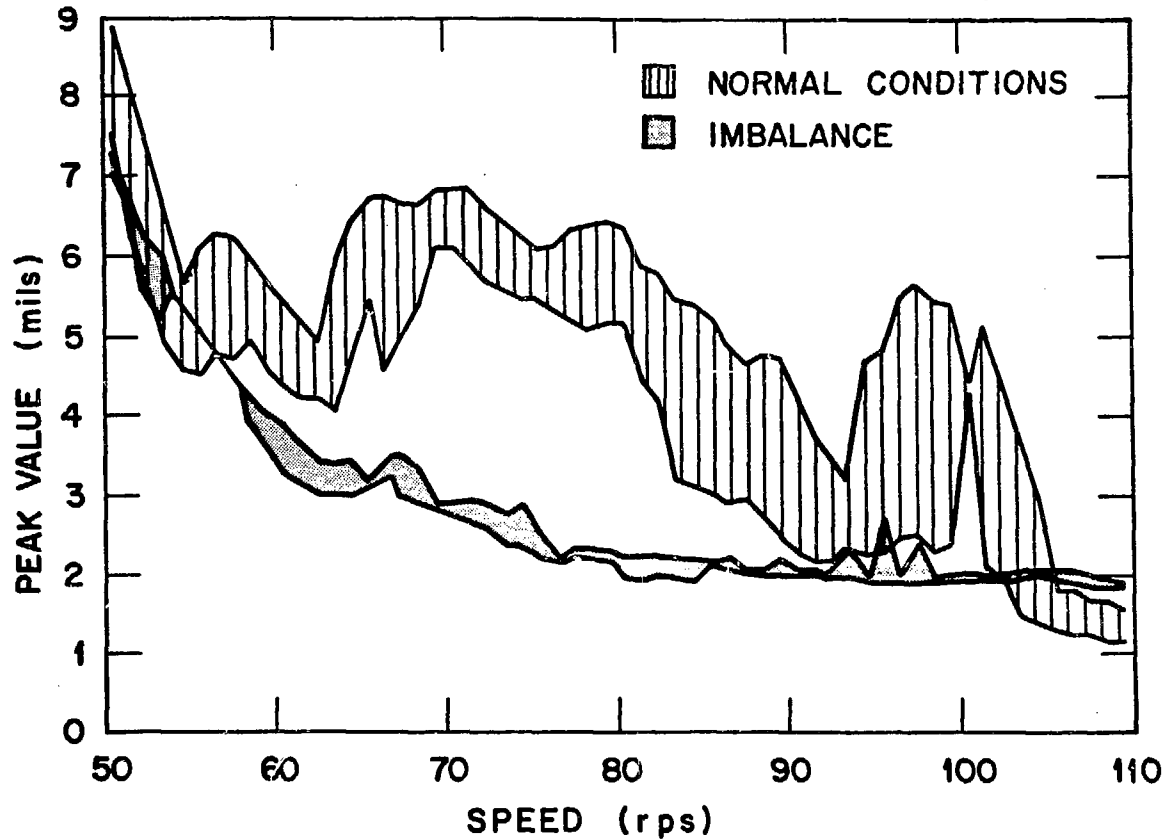


Fig. 4. The range of peak displacements for normal and imbalance conditions vs speed.

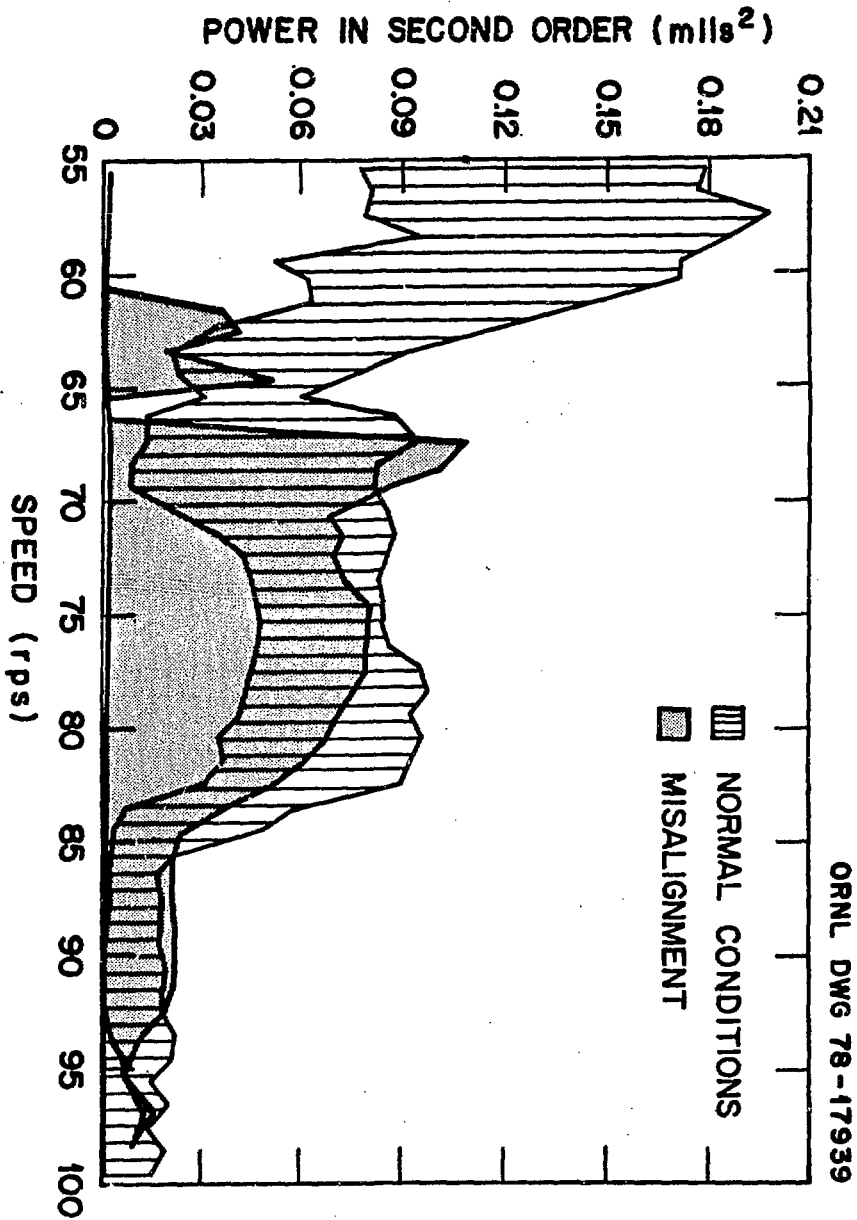


Fig. 5. The range of power estimates (displacement probe) at the second order for normal and misaligned conditions vs speed.

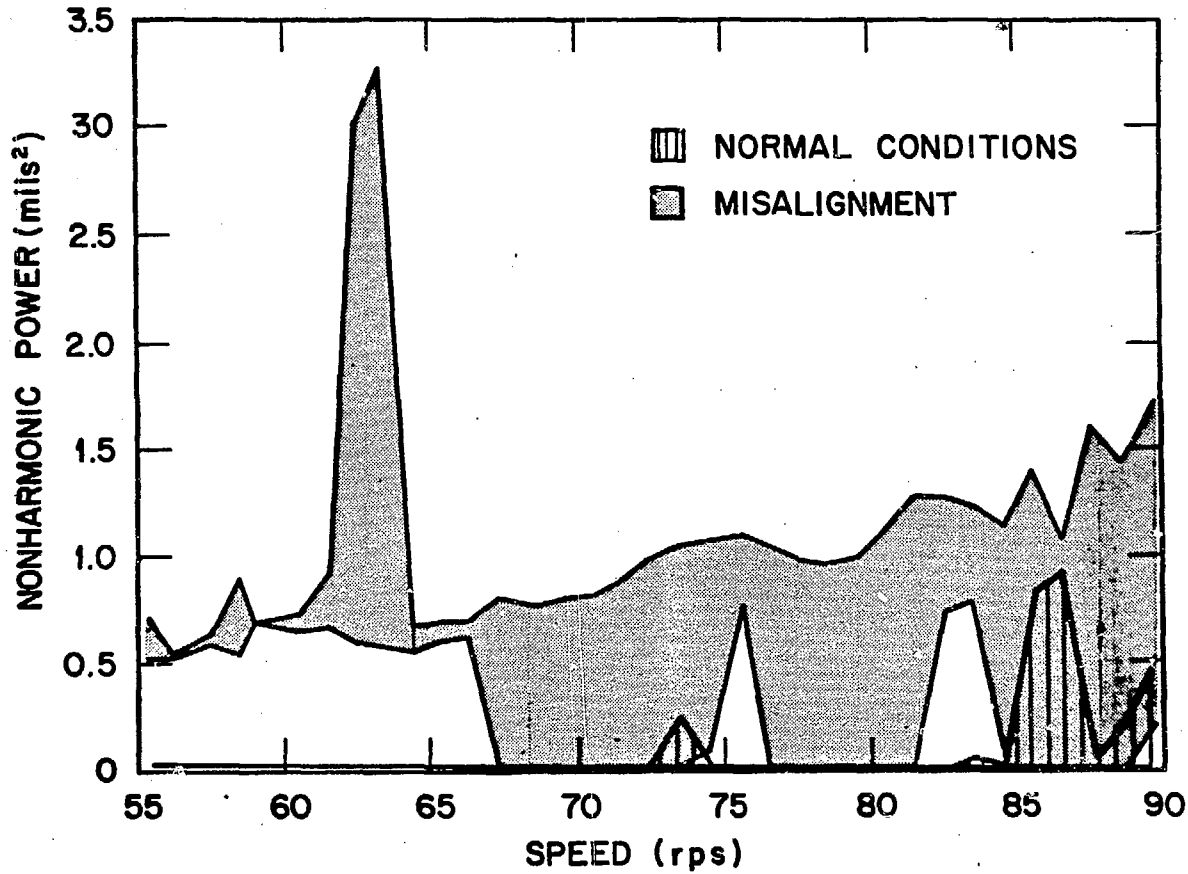


Fig. 6. The range of nonharmonic power estimates (displacement probe) for normal and misaligned conditions vs speed.

ORNL DWG 78-17940

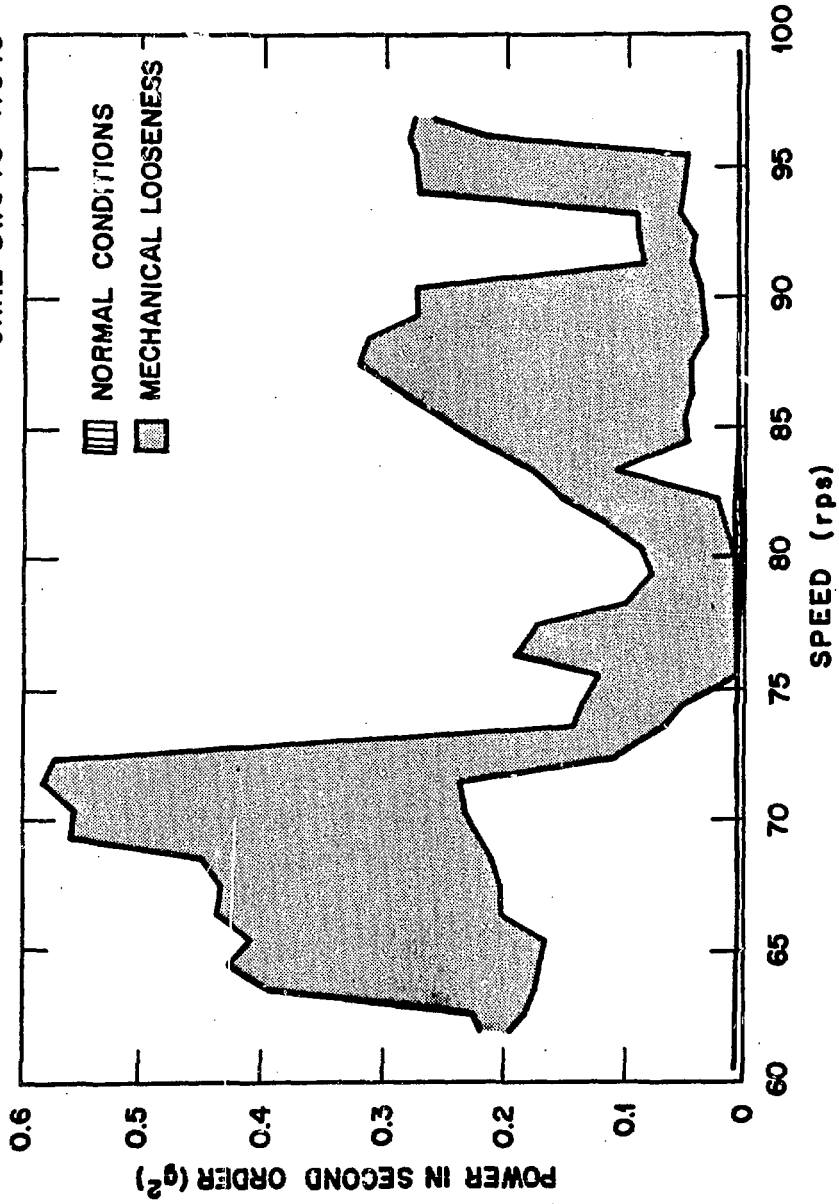


Fig. 7. The range of power estimates (accelerometer) at the second order for normal and mechanically loose conditions vs speed.

ORNL DWG 78-17937

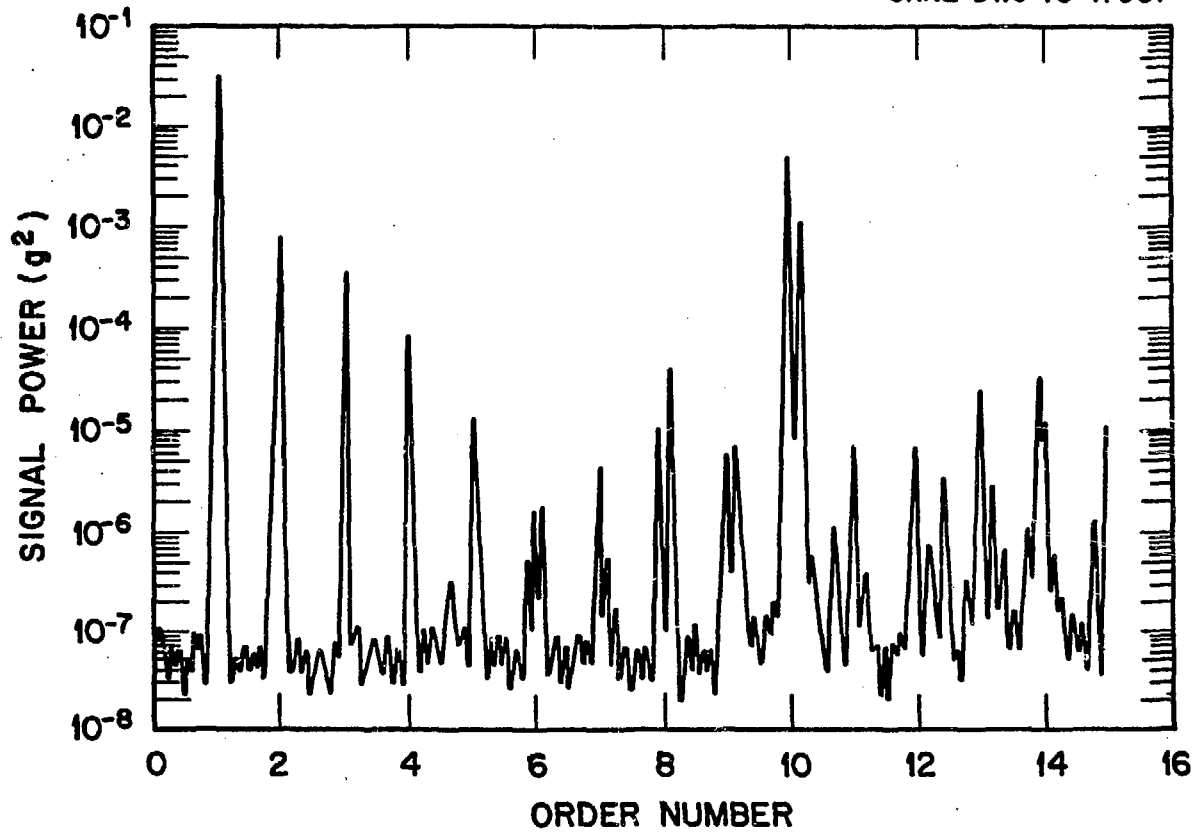


Fig. 8. Power spectrum of horizontal accelerometer during normal rotor operation at 59 rps.

ORNL DWG 78-17938

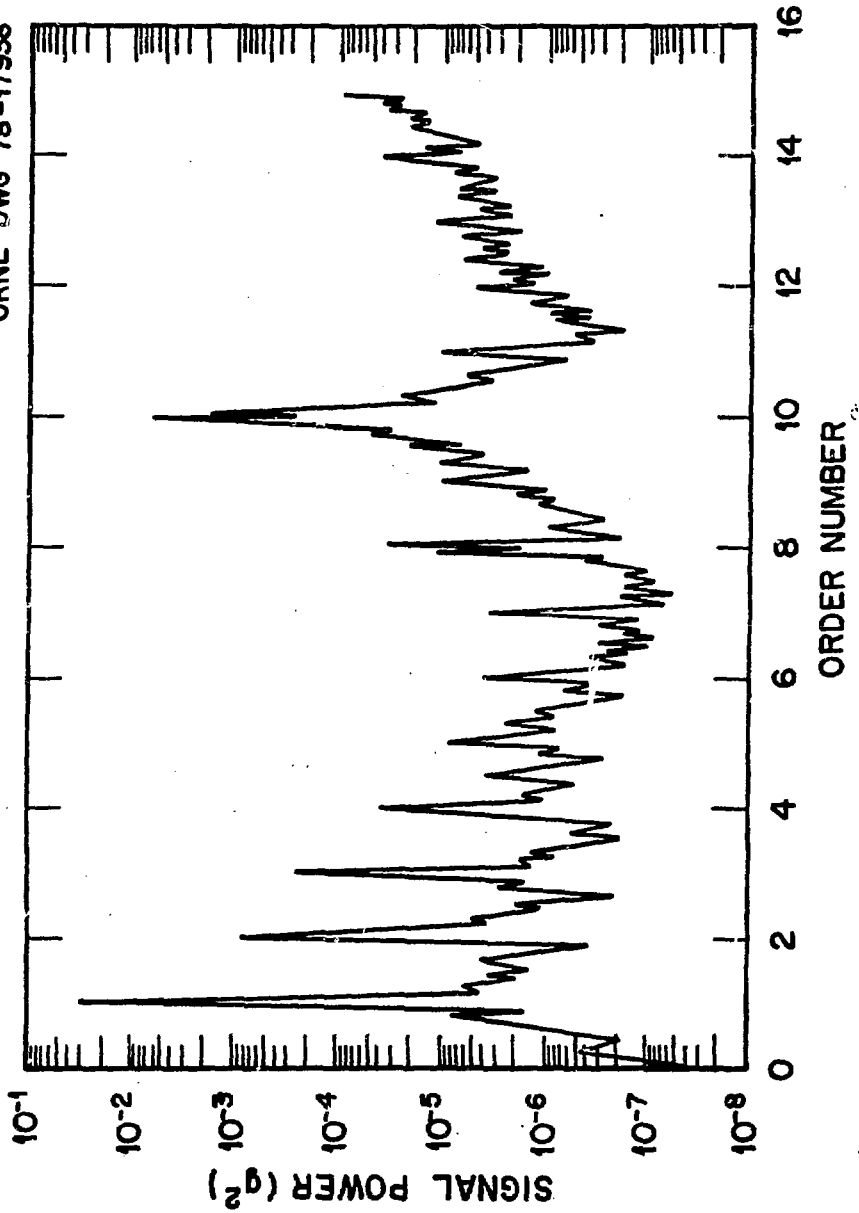


Fig. 9. Power spectrum of horizontal accelerometer during partial shaft rub test at 59 rps.

REFERENCES

1. M. P. Blake, "New Vibration Standards for Maintenance," *Hydrocarbon Processing and Petroleum Refiner*, January 1964, pp. 111-114.
2. R. L. Baxter and D. L. Bernhard, "Vibration Tolerances for Industry," ASME paper 67-PEM-14 for meeting April 10-12, 1967.
3. C. Jackson, "Vibration Measurement on Turbomachinery," *Chem. Engr. Progress*, V58, N3, March A72, pp. 60-65.
4. C. Jackson, "A Practical Vibration Primer -- Parts 1-8," *Hydrocarbon Processing*, April 1975-April 1978.
5. J. S. Mitchell, "Vibration Analysis -- Its Evolution and Use in Machinery Health Monitoring," *Society of Environmental Engineers Symposium on Machine Health Monitoring*, Imperial College, London, England, September 1975.
6. V. R. Dodd, "Spectral Applications for Petrochemical Plants," *Engineering Foundation Conf. on Applications of New Signature Analysis Technology*, July 1977.
7. Performance Monitoring and AIDS Seminar/Workshop, AERO Data, Inc., Washington, DC, September 20-24, 1976.
8. Bently-Nevada Machinery Protection Seminar, Cincinnati, Ohio, May 17-18, 1978.
9. H. P. Koehler, "Vibration Monitoring: Pumpset Reliability at Pickering GS," Ontario Hydro Report No. 574-11-K, February 1974.
10. M. M. Gupta and P. W. Davall, "Detection and Diagnosis of Incipient Failures in Cyclic Machines," *University of Saskatchewan, Saskatoon, Canadian Defense Research Board Grant 9781-04*, March 31, 1976.
11. E. Makay and O. Szamody, "Summary of Feed Pump Outages," EPRI-FP-754, April 1978.
12. R. James, B. Reber, B. Baird, and W. Neal, "Instrumentation of Predictive Maintenance Monitoring," *Mechanical Failure Prevention Group Proceedings, 22nd meeting, April 23-25, 1975*, pp. 114-127.
13. D. S. Wilson and J. L. Frarey, "Automated Machinery Surveillance and Diagnostics," *Progress in Nuclear Energy*, V 1, Pergamon Press, pp. 723-733 (1977).
14. "The ICEMS Story -- The U.S. Navy Inflight Engine Condition Monitoring System as Applied to the A7E Aircraft and the TF41-A-2 Engine," *Detroit Diesel Allison report EDR-8472*, April 30, 1975.
15. J. R. Passalacqua, "Description of an Automatic Gas Turbine TRENDS Diagnostic System," *ASME Gas Turbine Conf.*, March 1975.
16. Spectral Dynamics Machinery Vibration Seminar and Course Notes.
17. D. R. Houser and M. Drosjack, "Vibration Signal Analysis Techniques," *USAMRDL Technical Report No. 73-101*, December 1973.
18. R. P. Wallace and W. L. McCarthy, "VIDEC Ship Propulsion System Performance Monitor," *Mechanical Failure Prevention Group Proceedings, 22nd meeting, April 23-25, 1975*, pp. 221-257.
19. K. R. Piety, "Statistical Algorithm for Automated Signature Analysis of Power Spectral Density Data," *Progress in Nuclear Energy*, V 1, Pergamon Press, pp. 781-802 (1977).
20. E. Cortine, H. L. Engel, and D. K. Scott, "Pattern Recognition Techniques Applied to Diagnostics," *Society of Automotive Engr., Mid-Year Meeting, Detroit, Michigan, May 1970*.
21. L. F. Pau, "Adaptive On-Line Failure Diagnosis and Predictive Pattern Recognition," *Second International J. Conf. Pattern Recognition*, February 1974.
22. H. E. Hunter, "Demonstration of the Use of ADAPT to Derive Predictive Maintenance Algorithms for KSC Central Heat Plant," *Report No. AVSD-0084-73-RR, AVCO Systems Division for NASA, Wilmington, Mass., 01887*, November 1972.
23. Richard Woods, "An Investigation into Vibration Criteria for Rotary Machinery," *Ph.D. Thesis, University of Aston, Birmingham, England, 1968*.

APPENDIX

In Table A-1 is a list of the descriptors which we chose to include in our vibration signatures. Many of these descriptors are commonly used and require no additional explanation. However, the following discussion and equations should serve to clarify the descriptors we used.

Table A-1. Descriptors in vibration signature

1. Time-averaged waveform ("NPTS" values)
2. Lag value of time-average waveform
3. Shape factor for time-average waveform
4. Size factor for time-average waveform
5. Peak signal value
6. Total signal power
7. Harmonic power in signal
8. Nonharmonic power in signal
9. Average order of signal
10. Average harmonic order of signal
11. Average nonharmonic order of signal
12. Power at first order of signal
13. Power at second order of signal
14. Power at third order of signal
15. Phase of first order of signal
16. Phase of second order of signal
17. Phase of third order of signal

The waveform from a vibration sensor attached to a rotating machine has a repetitive component. Regardless of magnitude of this component, its presence can be enhanced by time-averaging the waveform. This process requires that the raw signal be sampled at some integer multiple of the frequency of rotation, f_0 . These sampled values, $X(i\Delta t)$, are then averaged using the following formula

$$\bar{X}_1 = \frac{1}{NREV} \sum_{n=1}^{NREV} X(i\Delta t + nT) \quad (1)$$

(i = 0, 1, 2, ... NPTS-1)

where T is the period of rotation

$$T = NPTS \cdot \Delta t = \frac{1}{f_0} \quad (2)$$

This time-averaging technique is equivalent to applying a comb filter to the original signal which passes only the fundamental frequency and its harmonics. The time averaged waveforms from two sensors at 90° to each other can be used to obtain average orbital plots which describe the motion of the shaft centerline at the monitored position. The "NPTS" values (usually 30) that describe the averaged waveform, \bar{X}_1 , are correlated with the averaged waveform obtained initially as a baseline, \bar{X}_B , to derive three additional quantities. The shape factor is the maximum value obtained for the normalized correlation function, $H(J)$, which is defined by

$$H(J) = \frac{\sum_{i=1}^{NPTS} \bar{X}_{1+J} \cdot \bar{X}_B}{\left[\sum_{i=1}^{NPTS} \bar{X}_B^2 \sum_{i=1}^{NPTS} \bar{X}_1^2 \right]^{1/2}} \quad (3)$$

(J = 0, 1, 2, ... NPTS-1)

Values for \bar{X}_{1+J} beyond \bar{X}_{NPTS} are obtained by repeating the original waveform. The point $J = L$ where $H(J)$ is a maximum also defines the lag value, LAG, and the size factor, SZF, according to the following expressions:

$$LAG = L \cdot \left(\frac{360}{NPTS} \right); \quad (4)$$

$$SZF = \frac{\sum_{i=1}^{NPTS} \bar{X}_{1+L} \cdot \bar{X}_B}{\sum_{i=1}^{NPTS} \bar{X}_B^2} \quad (5)$$

When analyzing the vibrational signals from rotating machinery, order-domain analysis (instead of the more familiar frequency-domain) simplifies interpretation of results, especially when variable speed operation exists. The basic relationship that allows conversion between the two domains is

$$Q = \frac{f}{f_0}, \quad (6)$$

where f_0 is the fundamental rotational frequency.

Integral orders ($Q = 1, 2, 3$, etc.) occur at harmonics of the running speed. If the vibrational signal is analyzed for NREV revolutions, the minimum order resolution achievable is

$$\Delta Q = \frac{1}{NREV}. \quad (7)$$

The power at any order, Q_i , will be denoted by $G(Q_i)$, where $Q_i = i\Delta Q$, $i = 1$, NOC (number of orders calculated).

Thus the total power in the vibrational signal up to some desired order, Q_D , is obtained by summing

$$TPOW = \sum_{i=1}^K G(Q_i), \quad (8)$$

where

$$K = \frac{Q_D}{\Delta Q}. \quad (9)$$

The harmonic power in the signal can be obtained by summing the power spectrum estimates at integral orders:

$$HPOW = \sum_{m=1}^N G(m), \quad (10)$$

where N is the largest integer for which $Q_N \leq Q_D$.

The nonharmonic power is the difference of these two quantities

$$NHPOW = TPOW - HPOW \quad (11)$$

When combining power estimates over an order interval, another parameter of interest is the power-weighted average order. This parameter provides an indication of the order at which the power in the interval is concentrated. This is given by

$$ATO = \left[\frac{\sum_{i=1}^k Q_i^2 G(Q_i)}{\sum_{i=1}^k G(Q_i)} \right]^{1/2}. \quad (12)$$

Similarly the average harmonic order is given by

$$AHO = \left[\frac{\sum_{m=1}^N m^2 G(m)}{\sum_{m=1}^N G(m)} \right]^{1/2}, \quad (13)$$

and the average nonharmonic order is given by

$$\text{ANHO} = \left[\frac{\sum_{i=1}^k Q_i^2 G(Q_i) - \sum_{m=1}^N m^2 G(m)}{\sum_{i=1}^k G(Q_i) - \sum_{m=1}^N G(m)} \right]^{1/2} \quad (14)$$

All of the parameters defined above can be calculated from the time domain signal directly without the need for order domain transformations. The total power can be obtained by integrating the squared time signal:

$$\text{TPOW} = \frac{1}{T} \int_0^T \dot{x}^2(t) dt; \quad (15)$$

$$\text{TPOW} \approx \frac{1}{\text{NDAT}} \sum_{i=1}^{\text{NDAT}} \dot{x}_i^2 \approx \sum_{i=1}^k G(Q_i). \quad (16)$$

The total harmonic power can be obtained by integrating the time averaged waveform

$$\text{HPOW} \approx \frac{1}{\text{NPTS}} \sum_{i=1}^{\text{NPTS}} \dot{x}_i^2 \approx \sum_{i=1}^N G(m). \quad (17)$$

The sums of the squared orders, weighted by their power in Eqs. (12)-(14), are equal to integrating the square of the derivative of the time signal and the time-averaged signals, respectively:

$$\sum Q_i^2 G(Q_i) = \frac{1}{T} \int [X'(t)]^2 dt; \quad (18)$$

$$\sum Q_i^2 G(Q_i) \approx \frac{1}{\text{NDAT}} \sum_{i=1}^{\text{NDAT}} \left(\frac{x_i - x_{i-1}}{\Delta t} \right)^2 (\Delta t); \quad (19)$$

$$\sum m^2 G(m) \approx \frac{1}{\text{NPTS}} \sum_{i=1}^{\text{NPTS}} \left(\frac{x_i - x_{i+1}}{\Delta t} \right)^2 (\Delta t). \quad (20)$$